ELSEVIER

Sensors and Actuators 86 (2000) 39–44

SENSORS AND ACTUATORS A PHYSICAL

www.elsevier.nl/locate/sna

Damping of a vibrating beam

Jarmo Hietanen [a,b,c,*], Johan Bomer [b], Jacques Jonsmann [d], Wouter Olthuis [b], Piet Bergveld [b], Kimmo Kaski [a]

[a] *Laboratory of Computational Engineering, Helsinki University of Technology, P.O. Box 9400, Miestentie 3, FIN-02015 Espoo, Finland*
[b] *MESA Research Institute, University of Twente, P.O. Box 217, 7500 AE Enschede, Netherlands*
[c] *Speech and Audio Systems Laboratory, Nokia Research Center, P.O. Box 100, FIN-33721 Tampere, Finland*
[d] *Mikroelektronik Centret, Technical University of Denmark, Bldg. 345 east, DK-2800 Lungby, Denmark*

Received 24 August 1999; received in revised form 14 February 2000; accepted 21 February 2000

Abstract

This study examines the vibration in a beam with one fixed end. The set-up consisted of a beam with one end clamped and a rigid plate having the same thickness of the beam, located adjacent to the unfixed end of the beam. The gap between the beam and the plate varied from 4 to 128 μm depending on the length of the beam. From the system behaviour in the small signal regime it was concluded that the frequency ratio of the second and first allowed transverse vibrations is solely a function of the gap size. In the large signal regime energy flow to other vibration modes takes place due to nonlinear effects. These two effects together with the squeeze film damping in the studied structure could be applied in constructing a mechanically isolated and damped substrate plate for a micromechanical sensor, aimed to consumer applications.

Keywords: Vibrating beam; Damping; Fluid–structure interaction

1. Introduction

Most mechanical structures have a tendency to ring when subjected to external impulses. This is a troublesome phenomenon in mechanical sensors, in which intensive ringing can temporarily black out the sensor. Ringing can occur in the actual sensor structure or in the sensor housing. Besides any transient damping in the sensor itself, an extra damping zone can be arranged around the sensor to reduce the ringing effect. In addition to this traditional approach, new possibilities to solve this problem can be found in an approach integrating computational modelling with component and system design and materials knowledge [1–5].

An example in which the effects of an external impulse are harmful can be found from audio applications for the consumer market, where products must be designed to withstand impact and recover quickly from any transient type of impulse. For instance, traditional microphone capsules most often include a rubber boot that attenuates external impulses, handling noise as well as sealing the acoustical ports. In such an application one way of implementing a damping zone is to apply a floating sensor base, consisting of, for example, a vibrating beam under a rigid sensor element. By tuning this substrate structure to the appropriate mechanical bandwidth relative to that of the actual sensor element, a suitable damping construction is created. Transients that occur in an impact event can be very powerful, and thus nonlinear effects are easily generated in the beam. These nonlinear effects in a substrate structure can introduce mode coupling in which energy is shifted between different vibrational modes. As a result more vibrations are then excited, but the overall amplitude decreases.

In this paper vibrations in a 100-μm thick substrate beam are studied. The beam is fixed at one end and a rigid plate of the same thickness is adjacent to the unfixed end of the beam. The structure is presented in Fig. 1. In this case the air is sheared more by the edges of the beam and the plate than squeezed between the beam and the base of the structure. The air gap between the beam and the plate

* Corresponding author. Tel.: +358-9-451-5728; fax: +358-9-451-4830.
E-mail address: jarmo.hietanen@hut.fi (J. Hietanen).

0924-4247/00/$ - see front matter
PII: S0924-4247(00)00423-4

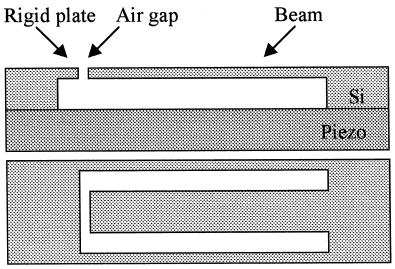

Fig. 1. A schematic cross-section (upper) and a top view (lower) picture of the vibrating beam and rigid plate.

varies from 4 to 128 μm. The rigid plate is used to generate nonlinear cross-talk between different vibration modes of the beam.

2. Theory

If the displacement and the curvature of a bar or beam are limited to the linear regime, the equation for the motion can be expressed as [6]

$$\frac{\partial^2 y}{\partial t^2} = -\kappa^2 c^2 \frac{\partial^4 y}{\partial x^4} \tag{1}$$

where y is the displacement of the beam for position x, c is the velocity of a transverse wave and κ stands for the geometrical cross-section parameter of the beam. In the case of a rectangular beam, $\kappa = t/\sqrt{12}$ where t is the beam thickness. A significant difference between this differential equation and a simpler second-order equation for the transverse waves in a string is the presence of a fourth partial derivative with respect to x. As a result of this difference, transverse waves occur with nonconstant velocity and changing shape [6,7].

After separation of the variables and using complex transverse displacement, which cancels time out from the exponential function, the general solution for a beam with one fixed end reduces to

$$y = \cos(\omega t + \phi)\left(A\left(\cosh\frac{\omega x}{\upsilon} - \cos\frac{\omega x}{\upsilon}\right) + B\left(\sinh\frac{\omega x}{\upsilon} - \sin\frac{\omega x}{\upsilon}\right)\right). \tag{2}$$

Here the phase speed of the transverse waves, $\upsilon = \sqrt{\omega c \kappa}$, is determined for a dispersive medium.

Applying the two boundary conditions (fixed and unfixed ends) to the equation the frequencies corresponding to the allowed modes of vibration are given by

$$f_n = \frac{\pi c \kappa}{8 L^2}(1.194^2, 2.988^2, 5^2, 7^2, \ldots). \tag{3}$$

Here L is the length of the beam. In the expression the numerical values in parentheses are specific for the vibration modes.

When the vibration modes in Eq. (3) are examined, it can be noticed that the ratio between the second and first modes is supposed to be a constant of 6.26 (unloaded case).

3. Sample fabrication and measurement set-up

The beams were fabricated using a dry-etching process from a 360-μm-thick silicon wafer that was polished on both sides. First the top side of the wafer was spin-coated with a positive photo-resist. After UV exposure the beam pattern was oxygen dry-etched more than 100 μm deep into the wafer. Then the top side of the wafer was covered with a polymer layer. After this the back side was spin-coated with photo-resist and UV exposed with an opening pattern so that the wafer would be thinner in places where there would be a beam, an opening or a plate. With this method the beams and plates were made equally thick. The back side was dry-etched until the beam and plate structure was approximately 100 μm thick. Finally the protective polymer layer was removed from the top side and the photo-resist layer was removed from the back side.

The beams had a width of 600 μm, and lengths varying from 4672 to 4796 μm. Due to the nature of the etching machine, the etching ratio was not uniform over the wafer, causing some thickness variation in the beam batches. Due to this the beams were divided into two sets according to thickness. Here the thinner beam set is called “A type” and the thicker beam set is called “B type”. The air gaps between the tip of the beam and the plate were measured as 4, 8, 16, 32, 64 and 128 μm. Scanning electron microscope (SEM) pictures showed that all of the cuts in the wafer were not exactly vertical, and due to this the gaps were slightly narrower than designed.

On both sides of the beam there were openings of 200 μm. Under the beam there was a 260-μm-thick air gap. As a result the structure closest to the beam is the rigid plate, located at the unfixed end of the beam. This way the squeeze film damping [8,9] under the beam is reduced to a minimum for small signal behaviour.

For vibration measurements a fibre-optics-based method was used [10,11]. Appropriate resolution was achieved by applying a simple geometrical optics method where the tip of an optical fibre illuminated the surface of the sample. The sample surface acts as a mirror and reflects part of the light back to the optical fibre. The amount of light reflected back into the fibre depends strongly on the fibre-to-surface distance, thus the vibration of the surface modulates the optical power reflected into the fibre. For a good signal-to-noise ratio (SNR) the fibre should be close to the surface.

In this case, a stable IR diode laser was used to illuminate one branch of a 2×2 optical fibre coupler, which conducted the incident light to the measuring branch [12]. The reflected light component from the sample sur-

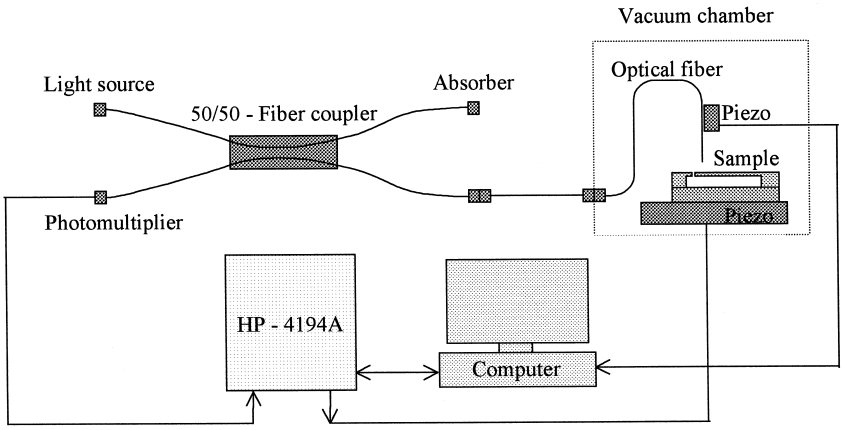

Fig. 2. Measurement set-up.

face was conducted to the sensing branch in which a photo-multiplier and basic operational preamplifier circuit converted the received signal for the analyser. In order to avoid extra reflections the free branch of the coupler was optically terminated. Taking into account the constraint of the SNR, the distance between the optical fibre and the beam was made as large as possible in order to utilise the maximum vibration amplitude of the beam and still avoid mechanical contact between these two components. Due to this arrangement any disturbance of the optical components due to vibration in the fluid was negligible. In Fig. 2 the core of the measurement set-up is illustrated.

In the measurement procedure the silicon sample was placed on top of a piezoceramic transducer. The frequency response of the actuating element was flat up to 200 kHz. The optical fibre was placed so as to measure the vibration of the tip of the beam. An HP-4194A Gain-Phase analyser was used to produce a sweep for sinusoidal excitation of the piezoceramic as well as to receive the vibration signal. The measurement system was computer controlled. The computer was used to control a separate piezo actuator on which the optical fibre was mounted. With this piezo actuator absolute displacement could be determined. Also, accurate resonance-peak and quality-factor calculations were performed. In the measurement system the ambient pressure could be adjusted from atmospheric pressure down to 0.01 mbar. The ambient pressures used were 1025 and 0.1 mbar. Under these conditions air still has a viscous nature [13].

4. Results

The fluid–structure interactions in the described beam-plate system can be classified into three regimes in terms of the vibration amplitude.

1. The vibration amplitude of the beam is limited to not exceed half of the beam thickness.
2. The vibration amplitude exceeds the thickness of the plate.
3. The vibration amplitude increases equal to the free distance under the beam.

In this study the vibration amplitudes were adjusted to meet the conditions of the 2nd and 3rd cases. For the last two cases a common factor is that the air is pumped from one side of the rigid plate to the other by the vibrating beam. In addition, in the 3rd case squeeze film damping and mechanical contact between the beam and the base of the system are present. Through these nonlinear effects mode coupling takes place in the beam. In mechanical microsensors and actuators the squeeze film damping is an important effect when the air gap is in the range of micrometres. Due to large openings at the beam sides and free distance under the beam, the squeeze film damping can be considered negligible for small vibration amplitudes.

The A-type beams met the conditions of the 2nd case (referred to above) and at the end the B-type beams fulfilled the 3rd case. The measured first vibration mode of the A-type beam was from 1.7 to 1.8 kHz. The measured second vibration mode of the A-type beam was from 10.9 to 12.3 kHz and the measured third vibration mode was from 30.9 to 35.1 kHz. In the frequency domain the overall effect of decreasing the ambient pressure from 1025 to 0.1

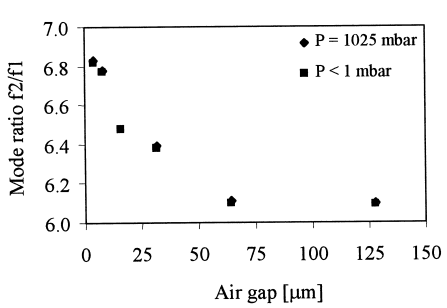

Fig. 3. Calculated frequency ratio of measured second and first resonances as the function of the air gap.

Table 1
The vibration mode data table of A-type beams. The beams had lengths varying from 4796 to 4672 μm and the effective thickness of 44 ± 4 μm. Effective thickness is average value based on measured resonance frequencies. Theory value is calculated by applying the effective thickness

First transverse mode (Hz)			Second transverse mode (Hz)			f_2/f_1 ratio		
Theory	Measured		Theory	Measured		Theory	Measured	
	0.1 mbar	1025 mbar		0.1 mbar	1025 mbar		0.1 mbar	1025 mbar
1805	1820	1806	11307	11077	11007	6.26	6.08	6.09
1808	1800	1785	11326	10971	10903	6.26	6.10	6.11
1815	1773	1760	11364	11317	11252	6.26	6.38	6.39
1827	1865	broken	11440	12087	12024	6.26	6.48	–
1851	1813	1802	11595	12281	12213	6.26	6.77	6.78
1903	1803	1792	11915	12303	12237	6.26	6.82	6.83

mbar was a resonance frequency shift for the first vibration mode from 11 to 15 Hz and for the second vibration mode from 63 to 70 Hz. In the case of the third vibration mode air load of ambient pressure dissipated the amplitude completely. In the amplitude domain the overall effect of decreasing the ambient pressure from 1025 to 0.1 mbar was a quality factor increase for the first vibration mode from 130–170 to 780–2500 and for the second vibration mode from 370–780 to 7500–12300. The measured first vibration mode for the B-type beam was from 2.5 to 2.8 kHz. In other respects, the characters of the B-type beam are similar when taking in consideration the slight frequency shift upwards. Based on the measured resonances and on Eq. (3), A-type beams were effectively 44 ± 4 μm thick and B-type were 65 ± 4 μm thick, indicating that the etching rate was greater than expected during the fabrication phase. This was independently verified also from SEM pictures.

In the 2nd vibration condition it was observed that the frequency ratio of the second and first vibration mode is a function of the air gap. According to Eq. (3) this is supposed to be a constant if other effects are not involved. This finding was independent of the ambient pressure change. It can also be observed that the measured ratio went below the theoretical value. This is due to the air load. In Fig. 3 the f_2/f_1 ratio as a function of the air gap is shown and in Table 1 vibration data related to the A-type beams is presented.

In this system attached air is moving along the beam. The moving beam generates a pressure field around itself. A pressure maximum is produced in front of the beam, leading to a pressure minimum being produced behind the beam [14]. The presence of the rigid plate modifies the generated pressure field. The plate cuts a part of the attached air from the tip of the beam and forces it partly behind the beam (Fig. 4). This partly fills in the pressure minimum. As a result, an extra air load occurs and the resonances are shifted towards lower frequencies. The fluid–structure interaction is stronger for more developed pressure fields. When the mode shapes of the vibrating beam are reviewed, it can be seen that with the same input energy the vibration amplitude at the unfixed beam end is larger for the first than for the second mode. Thus the proximity of a rigid plate would give a larger effect for the first mode compared to the second mode.

In the 3rd vibration condition nonlinear effects are involved. Typically this can be seen from the nonsymmetrical tilting of the resonance peaks. In addition to the previously described fluid–structure interaction the squeeze film damping, the mechanical contact between the beam and the base, and the elasticity of the structure, being a function of the vibration amplitude, are also involved. Under this condition pure narrow-band excitation breaks into several vibration modes. These vibration modes exchange energy between each other over time. In Fig. 5 the time-dependent mode coupling in the frequency domain is shown with a B-type beam.

In this measurement each of the vibration modes has its own vibration phase. Thus, if the narrow-band measurement system averages the signal over a sufficiently long time period, all energy conversion between the vibration modes is erroneously eliminated from the frequency response. As a result only the tilt in the resonance peak can be observed. However, the mode conversion still exists. By

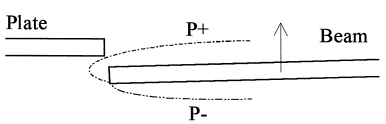

Fig. 4. A schematic pressure distribution around the tip of the vibrating beam.

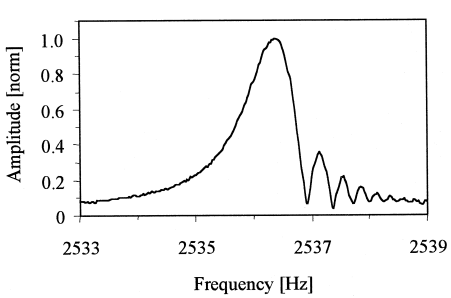

Fig. 5. Due to nonlinearities resonance peak tilts with large vibration amplitude. Pure vibration breaks to different vibration modes, which are changing energy between each other in time.

reducing the amount of averaging the phenomenon can be shown. The tilting and mode-coupling of the resonances depend on the direction of the frequency sweep.

In a real application the vibrating beam would be loaded at the unfixed end with the mass of the sensor element. Under this condition the position of the node point of the second vibration mode would move towards the mass. This further increases the coupling between the first and the second vibration modes. Thus the sensor element itself is driven towards rotational motion and the overall displacement is reduced. When the above-discussed principles of damping are used in an application, it should be noted that the beam dimensions must be optimised in order to meet the carrying capacity and other requirements of the system. For instance, the resonance frequency of the complete vibrating system should be adjusted to a frequency regime in which all disturbances are minimised. This can be done, for example, by choosing a suitable cross-section profile.

5. Conclusions

A system made up of a vibrating beam with one fixed end and a rigid plate was studied. In this system the plate interferes with generated fluid flow around the tip of the beam. It was observed that the frequency ratio of the second and first modes of vibration is a function of the air gap. Mode breaking at large vibration amplitudes was also observed.

From the application point of view, the effect of a narrow air gap together with mode-coupling could be applied as a damping zone under mechanical microsensors. The damping zone could counteract powerful external transients, which otherwise might damage or black out the sensor.

Acknowledgements

The authors thank Mr. B. Otter for performing the SEM study. The project was financed by the Academy of Finland and was supported by the Nokia Foundation.

References

[1] G.M. Sessler, Acoustic sensors, Sens. Actuators, A 25–27 (1991) 323–330.
[2] R. Schellin, Integrierte piezosensitive und kapazitive Ein-Chip-Silizium-Mikrofone, Dr. thesis, Techn. Univ. Darmstadt, Shaker Verlag, Germany, 1997, ISBN 3-8265-3333-X.
[3] M. Pedersen, A polymer condenser microphone realised on silicon containing preprocessed integrated circuits, Dr. thesis, University of Twente, Febodruk, the Netherlands, 1997, ISBN 90-365-0994-7.
[4] J. Hietanen, Integration of small transducers in commercial products, 16th ICA/135th ASA, Seattle, June 20th–26th, 1998, pp. 917–918.
[5] J. Hietanen, N. Zacharov, Method for implementation of an acoustic transducer, and an acoustic transducer, Nokia Mobile Phones, Finland. Patent application US-09/028,753, 1998.
[6] L.E. Kinsler, A.R. Frey, A.B. Coppens, J.V. Sanders, Fundamentals of Acoustics, 3rd edn., Wiley, New York, 1982, pp. 70–74.
[7] A.B. Wood, A Textbook of Sound, 3rd edn., Bell and Sons, London, 1964, pp. 111–118.
[8] M. Andrews, I. Harris, G. Turner, A comparison of squeeze-film theory with measurements on a microstructure, Sens. Actuators, A 36 (1993) 79–87.
[9] R.B. Darling, C. Hivick, J. Xu, Compact analytical modeling of squeeze film damping with arbitrary venting conditions using Green's function approach, Sens. Actuators, A 70 (1998) 32–41.
[10] A.D. Drake, D.C. Leiner, Fiber-optic interferometer for remote subangstrom vibration measurements, Rev. Sci. Instrum. 55 (1984) 162.
[11] D.A. Jackson, A. Dandridge, S.K. Sheem, Measurement of small phase shift using a single-mode optical-fiber interferometer, Optics Lett. 5 (1980) 139.
[12] J. Jonsmann, S. Bouwstra, Membrane parameter extraction from resonance frequencies,Eurosensors X, Leuven, Belgium, September 8th–11th, 1996, pp. 183–186.
[13] A. Fontel, J. Maula, R. Nieminen, C. Söderlund, K. Valli, A. Vehanen, M. Vulli, M. Ylilammi, Vacuum Technology — Tyhjiötekniikka, Insinööritieto, Finland, 1986, pp. 15–22, Chap. 1.
[14] S.F. Hoerner, Fluid–Dynamic Drag, Hoerner, NJ, USA, 1965, pp. 3.1–3.28, Chap. 3.

Biographies

Jarmo Hietanen received his PhD degree in physics from the University of Helsinki, Finland in 1996. He is a senior scientist at Nokia Research Center and senior researcher at the Helsinki University of Technology. In 1998–1999 he visited at the MESA Research Institute, University of Twente, the Netherlands. Dr. Hietanen's research interests are in the industrial areas of audio and ultrasound transducers.

Johan Bomer received the BSc degree in applied physics from the Hoger Technische School, the Netherlands in 1981. From 1983 until 1986 he worked as a technologist in the Semiconductor Physics Group of the University of Groningen. Since 1986 he has been working as a technologist in the Biosensor Technology Group, part of the MESA Research Institute, of the University of Twente.

Jacques Jonsmann received the MSc degree in 1995 from the Technical University of Denmark. He is currently working towards the PhD degree in microsystems at the Technical University of Denmark. His research interests are microactuators and resonant microstructures.

Wouter Olthuis received the PhD degree in electrical engineering from the University of Twente, the Netherlands in 1990. Currently he is working as an assistant professor in the Laboratory of Biosensors in MESA Research Institute, University of Twente. His research activity is in the field of physical and chemical sensors for biomedical applications.

Piet Bergveld received the PhD degree in electrical engineering from the University of Twente, the Netherlands in 1973 concerning the development of ISFETs. In 1984 he was appointed as Full Professor in Biosensor Technology of the University of Twente. Currently he is head of Laboratory of Biosensors in MESA Reseach Institute, University of Twente. He is a member of the Royal Dutch Academy of Science. The subject of his research is the further development of ISFETs and biosensors based on ISFET technology as well as physical sensors for biomedical and environmental applications.

Kimmo Kaski received the DPhil degree in theoretical physics from the University of Oxford, UK in 1981, after receiving the Licentiate of Technology degree in electrical engineering from the Helsinki University of Technology, Finland in 1977. In 1987 he was appointed as Full Professor in Microelectronics of the Tampere University of Technology. In 1996 he was appointed as Full Professor in Computational Engineering of Helsinki University of Technology and at the same time the Academy Research Professor for Computational Science and Engineering of the Academy of Finland. Currently he is the head of the Research Centre for Computational Science and Engineering at Helsinki University of Technology. He is a fellow of both the American Physical Society (USA) and the Institute of Physics (UK). His research interests are in the field of computational materials research and computational information technology.